Volume 16
Number 46
14 December 2025
Pages 21645–22176

Chemical Science

rsc.li/chemical-science

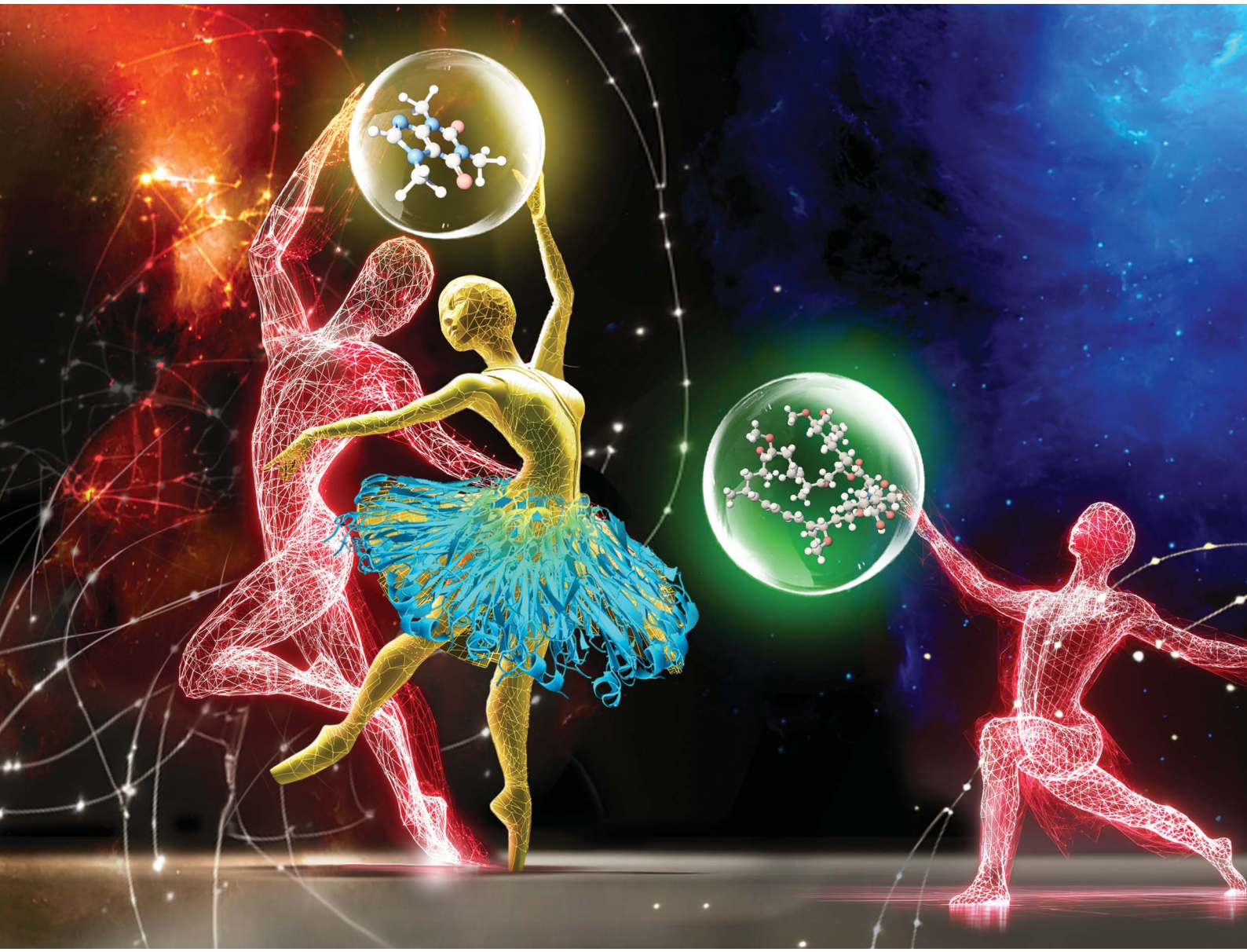

ISSN 2041-6539

ROYAL SOCIETY OF CHEMISTRY

EDGE ARTICLE
Lian He, Yubin Zhou *et al.*
Reprogramming chemically induced dimerization systems with genetically encoded nanobodies

15 YEARS ANNIVERSARY

Chemical Science

ROYAL SOCIETY OF CHEMISTRY

EDGE ARTICLE

View Article Online
View Journal | View Issue

Cite this: *Chem. Sci.*, 2025, **16**, 21774

All publication charges for this article have been paid for by the Royal Society of Chemistry

Received 29th July 2025
Accepted 17th October 2025

DOI: 10.1039/d5sc05703e

rsc.li/chemical-science

Reprogramming chemically induced dimerization systems with genetically encoded nanobodies

Tianlu Wang,†[a] Tatsuki Nonomura,†[a] Mingguang Cui,[a] Tien-Hung Lan,[a] Pauline X. Cai,[a] Lian He*[a] and Yubin Zhou *[ab]

Chemically induced proximity (CIP) systems harness small molecules to control protein–protein interactions, thereby enabling remote control over physiological processes and advancing the development of smart and personalized therapies. While substantial efforts have focused on developing new chemical inducers for tailored CIP applications, repurposing established systems to confer novel functions remains a highly cost-effective and efficient strategy. In this study, we employed genetically encoded nanobodies to overcome key bottlenecks of two widely used CIP systems in specific biological contexts. By incorporating the bivalent COSMO module and UniRapR into an anti-mCherry nanobody, we reprogrammed the homodimeric COSMO system into a caffeine-inducible heterodimerization system and transformed the classic rapamycin-dependent ON switch into an OFF switch, thereby conferring new functionality of the existing chemogenetic toolkit and expanding the repertoire of CIP technologies.

Introduction

Chemically induced proximity (CIP) systems have transformed biomedical research by enabling precise, tunable, and reversible control of protein activity and cellular functions.[1] Most current CIP tools exploit the hetero- or homodimerization of genetically encoded modules to regulate gene expression, protein dynamics, genome organization, and therapeutic cell engineering.[2–8]

The most widely used CIP system is based on rapamycin-induced heterodimerization between FKBP12 and the FRB domain of mammalian target of rapamycin (mTOR).[9–11] Another representative system, COSMO (a caffeine-operated synthetic module), uses the widely consumed caffeine molecule to trigger homodimerization between two caffeine-operated synthetic modules.[12] These two systems exemplify two typical classes of CIP tools and have been applied in diverse biomedical contexts. However, both approaches have inherent limitations. The COSMO system is less effective for applications that require heterodimerization. For the FRB-FKBP system, most efforts have focused on enhancing switchable association or allosteric control through engineering of FRB-FKBP variants (*e.g.*, UniRapR[13,14] and cpRAPID[15]) or designing alternative rapalogs (*e.g.*, iRap,[16] AP21967,[17] and cRap[18]) as the chemical switches. Yet, no rapamycin-based dissociation systems have been reported, restricting the full potential of this otherwise versatile CIP platform.[19]

To address these unmet challenges, we established a versatile platform based on genetically encoded nanobodies to reprogram COSMO into a caffeine-inducible heterodimerization system and UniRapR into a rapamycin-switchable dissociation system. Although nanobodies have been engineered to create various chemical-responsive genetically encoded proteins[20] or directly conjugated with small molecules to modulate endogenous targets,[21] they have not previously been explored as a platform to overcome key limitations existing in some current CIP tools and thereby expand their utility in biological applications. By inserting a bivalent COSMO module with a flexible linker (biCOSMO-L)[12] into the mCherry-specific nanobody LaM8, caffeine could induce heterodimerization between the engineered nanobodies and mCherry, thereby converting the homodimeric COSMO system into a heterodimeric CIP tool. We further applied this heterodimeric system to modulate tyrosine receptor kinase signalling and downstream customized gene expression, effectively eliminating the basal toxicity observed when COSMO was used as a homodimeric tool in caffeine-controlled receptor signalling. In parallel, by inserting the UniRapR module at distinct positions within the nanobody, we designed a variant that converts rapamycin responsiveness from mediating association to driving dissociation of targeted modules, thereby filling a critical gap in expanding the classical FRB-FKBP-based CIP system.

[a]*Centre for Translational Cancer Research, Institute of Biosciences and Technology, Texas A&M University, Houston, TX 77030, USA. E-mail: lhetamu@gmail.com; yubinzhou@tamu.edu*

[b]*Department of Translational Medical Sciences, College of Medicine, Texas A&M University, Houston, TX 77030, USA*

† These authors contributed equally.

Results

Inspired by our group and others on engineering nanobodies as an optogenetic ON-switch[22–25] and exploiting biCOSMO-L as an allosteric switch,[12] we hypothesized that LaM8 could be allosterically switched by caffeine through insertion of biCOSMO-L. To identify caffeine-responsive variants, we first established a cytoplasm-to-mitochondria translocation assay (Fig. 1a). In this setup, mCherry was anchored to mitochondrial outer membrane (Mito-mCh), while engineered LaM8 variants were expressed in the cytosol. Caffeine-induced translocation was quantified by monitoring GFP intensity changes on mitochondria, allowing direct comparison of the response of LaM8 variants.

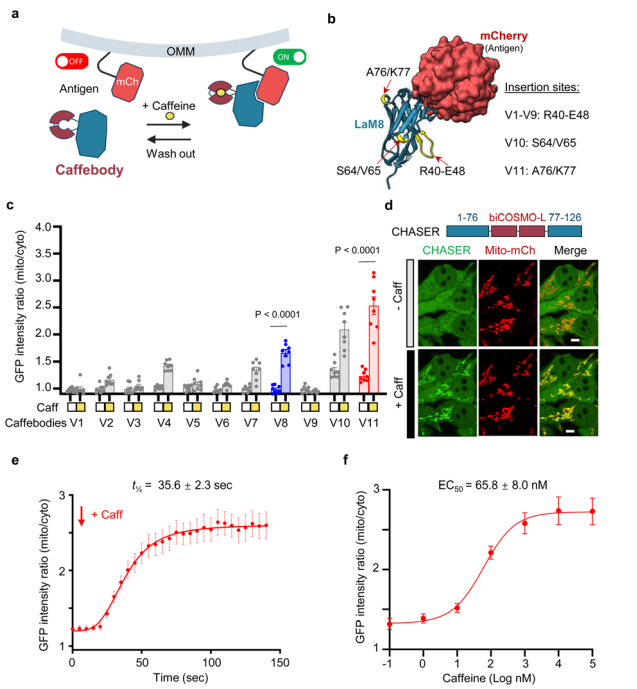

Fig. 1 Design of a caffeine-switchable heterodimerization system leveraging genetically encoded nanobodies. Data are presented as mean ± sem. (a) Schematic illustration of the design and a mitochondria (Mito) translocation assay used to screen the caffeine-switchable heterodimerization system. (b) The 3D structure (left) illustrates the interaction between LaM8 and mCherry (PDB entry: 8IM0). Two tandemly linked COSMO modules (biCOSMO-L) were inserted at distinct positions (highlighted in yellow) located within flexible loops of LaM8, an anti-mCherry nanobody, to yield Caffebody variants. Different insertion sites corresponding to the Caffebody variants V1–V11 are shown on the right. (c) Quantification of caffeine-inducible changes in the binding between Mito-mCh and 11 versions of anti-mCh Caffebodies. (d) Confocal images of HeLa cells showing the colocalization between the antigen (Mito-mCh; red) and Caffebody-V11 (termed as CHASER) before and after 10 μM caffeine treatment. Quantification data are shown in Fig. 1c. The domain architecture of CHASER was shown above the images. Scale bar, 5 μm. (e) Quantification of chemical inducible changes in the binding between Mito-mCh and anti-mCh CHASER upon caffeine addition within 2.5 min. $n = 8$ cells from three independent biological replicates. (f) Dose–response curve of CHASER expressed in HeLa cells. The Mito-to-cytosol ratios of GFP intensity was plotted against escalating doses of caffeine. $n = 8$ cells from three independent biological replicates.

To minimize perturbation of the mCherry-LaM8 interaction interface, we selected 11 insertion sites located on flexible loops of LaM8 opposite to the complementarity-determining regions (CDRs), generating a library of variants termed "Caffebodies V1–V11" (Fig. 1b). Remarkably, six of the 11 variants (V2, V4, V7, V8, V10, and V11) exhibited appreciable caffeine-induced responses in the translocation assay, with translocation ratio changes ranging from 17% to 104%, while maintaining minimal basal interaction in the absence of caffeine. Among these, Caffebody-V11 showed the highest translocation ratio change (104%) and was designated as CHASER (caffeine-induced heterodimerization *via* anti-mCherry nanobody scaffold engineering and reprogramming) (Fig. 1c and d). Notably, Caffebody-V8 may serve as an alternative for applications requiring minimal basal activity but moderate inducibility, as it displayed the lowest background and moderate caffeine-induced translocation (68%) (Fig. 1c, and S1, SI).

Since CHASER proved to be a robust caffeine-dependent heterodimerization tool, we further characterized its kinetics, reversibility, and EC_{50} (Fig. 1e, f, and S2, SI). Compared to COSMO, CHASER exhibited a similar activation half-life upon caffeine addition (29.4 ± 1.6 s for COSMO[12] *vs.* 35.6 ± 2.3 s for CHASER; Fig. 1e) but showed slower reversibility upon caffeine washout (83.1 ± 1.1 s for COSMO[12] *vs.* 14.8 ± 5.1 min for CHASER; Fig. S2, SI). This delayed reversibility likely reflects the two-step requirement for CHASER: first disrupting its intramolecular interaction of biCOSMO-L, followed by dissociation of CHASER from mCherry. In addition, the slow off-rate may result from a slower conformational change of the nanobody from its active to inactive state after caffeine dissociation. Despite the slower reversibility, CHASER demonstrated a lower EC_{50} (65.8 ± 8.0 nM) compared to COSMO (95.1 ± 1.2 nM; Fig. 1f),[12] consistent with the high efficiency of forming intramolecular interactions in CHASER relative to the intermolecular dimerization required for COSMO.

We next explored whether caffeine-containing beverages could modulate the CHASER-antigen interaction in live cells using the same mitochondria-translocation assay as a readout. Indeed, the addition of diluted coffee, tea, soda, or energy drinks (such as red bull) to the culture medium induced varying degrees of cytosol-to-mitochondria translocation (Fig. S3a, SI). Moreover, methylxanthines, such as theophylline-a caffeine analogue widely used clinically for asthma and chronic obstructive pulmonary disease[26,27]-similarly activated CHASER (Fig. S3b, SI). Importantly, we observed a strong positive correlation between the relative translocation response and the caffeine content of the tested beverages (Fig. S3c, SI). Taken together, CHASER represents an efficient and highly sensitive heterodimerization CIP tool that can be readily activated by caffeine or caffeine-containing beverages, offering enhanced sensitivity and tuneable kinetics.

Having established a robust heterodimerization CIP tool, we next sought to address a key challenge in biological applications-the unwanted basal activation caused by COSMO-mediated homodimerization. Previously, we attempted to use COSMO to induce dimerization of a plasma membrane (PM)-tethered intracellular kinase domain derived from receptor

tyrosine kinases (RTKs, RTK-ICD) upon caffeine addition to control downstream signaling.[12] However, we observed constitutive RTK activation even in the absence of caffeine, consistent with previous reports on optogenetically controlled RTKs.[28,29] The constitutive basal activity may arise from the tendency of myristoylated or palmitoylated RTK-ICDs, when fused to chemo- or opto-controlled components and anchored to the plasma membrane, to cluster within lipid-rich microdomains, where the resulting high local density of engineered receptors and signalling partners drives activation in the absence of external stimulation.

To circumvent this issue, we adopted a heterodimerization strategy. Tetramerized mCherry (TD-mCh) was anchored on the plasma membrane (PM), while the intracellular TrkA kinase domain (TrkA-ICD) was fused to CHASER (termed Caf-TrkA) and expressed in the cytosol, thereby preventing basal activation in the absence of ligand. Upon caffeine addition, Caf-TrkA was expected to heterodimerize with PM-anchored TD-mCh, leading to its membrane recruitment, oligomerization, and subsequent activation of downstream effectors *via* the phospholipase Cγ (PLCγ) and MAPK/ERK pathways[29] (Fig. 2a and b). Indeed, caffeine treatment induced a robust increase of cytosolic Ca^{2+}, evidenced by a 4.8-fold increase in the GCaMP6s fluorescence (Fig. 2c and d), confirming inducible activation of the PLCγ pathway. We further monitored ERK signalling using a synthetic kinase activity relocation sensor (ERK-SKARS),[30] which translocates from the nucleus to the cytosol upon ERK-mediated phosphorylation of nuclear localization sequences (NLS). In HeLa cells expressing Caf-TrkA and TD-mCh, caffeine addition markedly increased ERK phosphorylation (Fig. S4, SI) and induced pronounced nuclear export of the ERK sensor (Fig. 2e and f), indicating activation of the MAPK/ERK pathway.

We then harnessed the CHASER-TrkA-ICD platform to drive tunable gene expression under the control of Ca^{2+}/MAPK/ERK-responsive elements, including serum response element (SRE), NFAT response element (NFAT-RE), and cAMP response element (CRE).[31] Upon caffeine stimulation and activation of both PLCγ and ERK pathways, we observed a 7.7-fold increase in GFP fluorescence (Fig. 2g and h), while maintaining minimal basal fluorescence prior to caffeine treatment.

Collectively, this heterodimerized CIP design enabled caffeine-inducible activation of RTK signalling cascades while effectively eliminating the basal activity observed with COSMO-based RTK designs.

To further establish CHASER as a broadly applicable CIP system, we next tested whether it could achieve comparable functional outcomes to the homodimeric COSMO system in previously demonstrated biological applications. Specifically, we explored whether CHASER could gate Ca^{2+} channels and control Ca^{2+}-dependent gene transcription *via* the nuclear factor of activated T cells (NFAT) pathway, similar to COSMO.[12] We selected the Ca^{2+} release-activated Ca^{2+} (CRAC) channel as our engineering target. CRAC channels consist of two essential components: stromal interaction molecule 1 (STIM1),[32–35] which senses ER Ca^{2+} depletion and gates the ORAI1 channel, the pore-forming subunit mediating Ca^{2+} influx across the plasma membrane.[36,37] Forced apposition of the N-terminal coiled-coil region 1 (CC1) of the cytoplasmic domain of STIM1 (STIM1ct) can relieve its autoinhibitory conformation and directly activate ORAI channels. Therefore, we reasoned that caffeine-induced heterodimerization between CHASER-STIM1ct and mCh-STIM1ct would activate endogenous ORAI channels (Fig. S5a, SI). Indeed, upon caffeine treatment, HeLa cells co-expressing both CHASER-STIM1ct and mCh-STIM1ct exhibited a marked increase in Ca^{2+} influx (Fig. S5b, SI), accompanied by robust nuclear translocation of NFAT-GFP (Fig. S5b, SI). Consequently,

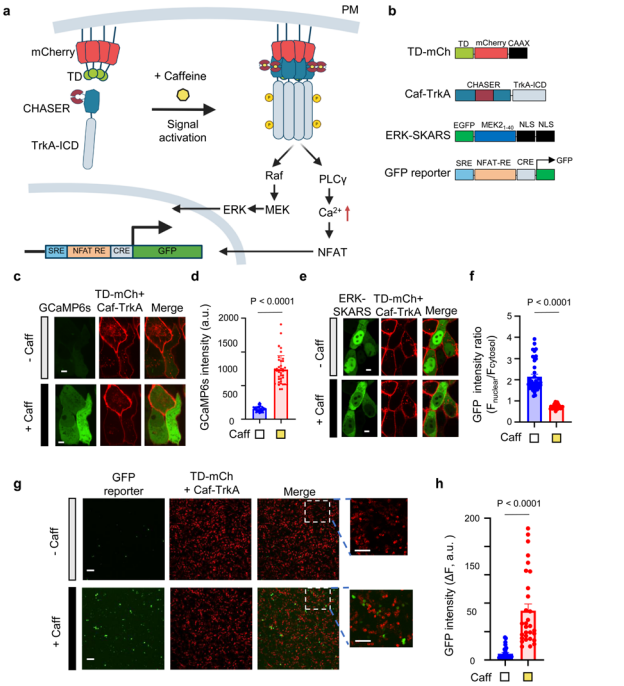

Fig. 2 CHASER applied for caffeine-induced activation of TrkA signalling and targeted gene expression. Data are presented as mean ± sem. (a) Schematic illustrating the use of CHASER for caffeine-induced TrkA activation *via* conditional heterodimerization between the intracellular kinase domain (TrkA-ICD) and a tetramerized mCherry (TD-mCh) anchored to the plasma membrane (PM). (b) Constructs used in the assays depicted in panel a. (c) Confocal imaging of GCaMP6s fluorescence (green) in HeLa cells coexpressing TD-mCh and Caf-TrkA to monitor Ca^{2+} influx through the caffeine-induced activation of the downstream phospholipase C gamma (PLCγ) pathway. Scale bar, 5 μm. (d) Quantification of cytosolic Ca^{2+} changes following caffeine addition. $n = 40$ cells from three independent biological replicates. (e) Confocal imaging to monitor ERK activation *via* the MAPK/ERK pathway in HeLa cells co-expressing the indicated constructs upon caffeine stimulation. ERK phosphorylation masks the NLS motifs in ERK-SKARS (green), promoting its nuclear export to the cytosol. (f) Quantification of the nuclear exit of ERK-SKARS in HeLa cells co-expressing the indicated constructs, as shown in Fig. 2e $n = 40$ cells from three independent biological replicates. (g) Confocal images showing EGFP reporter expression before and after caffeine treatment. HEK293T cells were co-transfected with the indicated constructs along with a GFP reporter driven by three synthetic transcriptional response elements (REs). Areas within the white boxes were enlarged and shown beside the whole cell image. Scale bar, 100 μm. (h) Quantification of GFP fluorescence intensity in HEK293T cells co-expressing the indicated constructs and treated with increasing concentrations of caffeine. $n = 30$ cells from three independent biological replicates.

we observed strong caffeine-induced expression of a luciferase reporter gene driven by NFAT response elements (Fig. S5c, SI). As a control, the low caffeine dose used in our assay neither triggered appreciable Ca^{2+} influx (Fig. S5b, SI) nor induced Ca^{2+}-dependent reporter gene expression in HEK293 cells co-expressing CHASER and mCh-STIM1ct alone (Fig. S5c, SI).

Collectively, these results further support that CHASER functions as an effective CIP tool for biological applications beyond those achievable with COSMO, enabling precise control of Ca^{2+} signalling and downstream gene expression.

Since the classical FRB-FKBP system functions as a rapamycin (or rapalog)-inducible association system, expanding its utility to include ligand-induced dissociation would greatly broaden its potential biological applications (Fig. 3a). Upon analysing the predicted 3D structure of UniRapR inserting into LaM8,[38] we found that its N- and C-termini form two tightly packed β-sheets (Fig. 3b), in contrast to LaM8 variant inserted with biCOSMO-L, whose N- and C-termini consist of flexible linkers and two β-sheets belonging to separate COSMO modules that remain non-interacting in the absence of caffeine (Fig. S6, SI).[12] This structural difference explains their distinct allosteric behaviours: in biCOSMO-L, caffeine triggers intramolecular COSMO interactions, stabilizing a tighter conformation that activates engineered LaM8; in contrast, inserting UniRapR into LaM8 is predicted to minimally perturb its basal interaction, while rapamycin binding could bring the domains closer to the interaction interface between engineered LaM8 and mCherry, thereby disrupting the interaction and initiating dissociation.

To test this idea, we employed the same cytoplasm-to-mitochondria translocation assay previously used for CHASER to engineer 11 LaM8 variants, simply by replacing biCOSMO-L with UniRapR to generate a library termed "Rapabodies V1–V11". Mitochondrial GFP fluorescence was measured before and after rapamycin treatment. Among these variants, Rapabodies V1–V9 showed no appreciable response, while Rapabody-V10 exhibited only a modest increase in binding to mitochondria-anchored mCherry (Fig. 3c). Notably, Rapabody-V11 displayed tight binding to mitochondria-tethered mCherry, which was efficiently dissociated by rapamycin, resulting in a 59% reduction in mitochondrial GFP fluorescence (Fig. 3c and d). Owing to this unique rapamycin-triggered dissociation property, we designated this optimized variant RASER (rapamycin-induced dissociation *via* anti-mCherry nanobody scaffold engineering and reprogramming).

We next characterized RASER's biophysical properties. RASER displayed rapid dissociation kinetics, with a half-life of 26.9 ± 2.1 s (Fig. 3e), and an effective concentration (EC_{50}) of 172.1 ± 14.2 nM in mammalian cells (Fig. 3f). Taken together, we successfully developed the first rapamycin-induced dissociation system, RASER, which combines fast activation kinetics with efficient induction at low ligand concentrations, thereby expanding the functional repertoire of rapamycin-based CIP tools.

With this unique rapamycin-induced dissociation system in hand, we next evaluated its potential for broader biological applications. CRISPR activation (CRISPRa) systems have been widely utilized for transcriptional activation,[39,40] and the

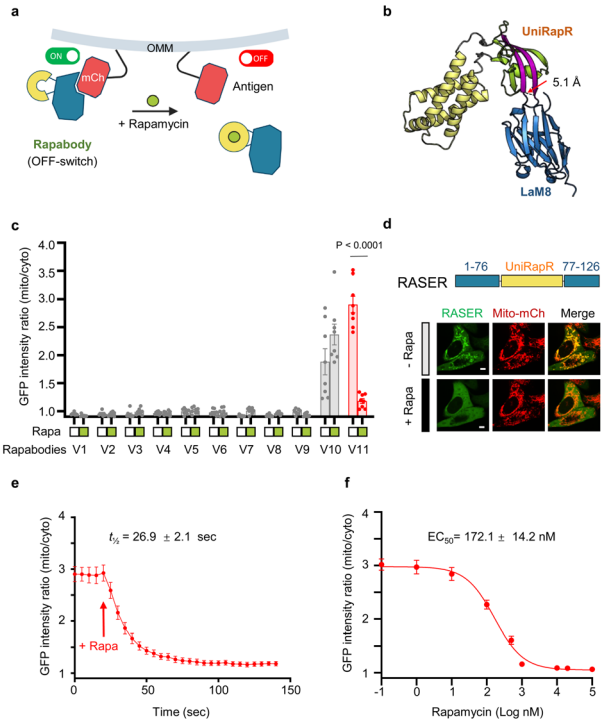

Fig. 3 Design of a rapamycin-switchable dissociation system leveraging genetically encoded nanobodies. Data are shown as mean ± sem. (a) Schematic illustration of the design and the mitochondria translocation assay used to screen the rapamycin-switchable OFF system. (b) The 3D structure predicted by AlphaFold illustrates the structure of UniRapR inserted into the LaM8 scaffold (designated Rapabody) in the absence of rapamycin. (c) Quantification of rapamycin-inducible changes in the binding between Mito-mCh and 11 versions of anti-mCh Rapabodies. (d) Confocal images of HeLa cells showing the colocalization between the antigen (Mito-mCh; red) and Rapabody-V11 (termed as RASER; green) before and after treatment with 10 μM rapamycin. Quantification data are shown in Fig. 3c. The domain architecture of RASER (Rapabody-V11) was shown above the corresponding images. Scale bar, 5 μm. (e) Quantification of rapamycin-inducible changes in the binding between Mito-mCh and anti-mCh RASER. The corresponding half-lives were indicated. $n = 8$ cells from three independent biological replicates. (f) Dose–response curve of RASER expressed in HeLa cells. The Mito-to-cytosol ratios of GFP intensity were plotted against escalating doses of rapamycin. $n = 8$ cells from three independent biological replicates.

classical FRB-FKBP dimerization module has been incorporated into split dCas9 architectures to achieve rapamycin-inducible gene activation, providing temporal control while mitigating potential toxicity and off-target effects.[41] However, a complementary rapamycin-inducible transcriptional deactivation system remains lacking, which would further expand the utility of CIP tools in the CRISPR field-particularly given the limited reversibility of the FRB-FKBP system.[3,42] Rapamycin-inducible activation systems are most effective when strict control over the initiation of dCas9 activity is required; however, once activated, CRISPRa remains constitutively active and is difficult to shut down due to the poor reversibility of rapamycin. In this respect, rapamycin-inducible transcriptional deactivation systems provide the ability to terminate activity on demand,

thereby further reducing undesired toxicity and potential off-target effects.

To address this need, we tested whether RASER could provide rapamycin-controlled assembly of a functional CRISPRa complex. Specifically, we fused mCherry to dCas9 and RASER to the transcriptional activator VP64 (Fig. 4a). As anticipated, rapamycin treatment triggered efficient dissociation of RASER-VP64 from mCh-dCas9, resulting in a pronounced suppression of reporter gene expression (TagBFP), with an 85% reduction in BFP fluorescence intensity. In contrast, cells expressing a non-rapamycin-responsive LaM8-VP64 control showed no significant change in reporter expression before or after rapamycin treatment (Fig. 4b and c). To further validate this RASER-CRISPRa system, we continued to explore its utility in modulating the expression of endogenous genes. We chose Long interspersed element-1 (LINE-1) retrotransposons as the target gene, as it accounts for nearly 20% of the human genome and is implicated in diverse pathophysiological processes, including aging, cancer, and neurological disorders.[43] Applying the rapamycin-controlled CRISPRa method to study the activation and subsequent deactivation of LINE-1 elements can further facilitate our understanding of LINE-1 function.[44] As expected, rapamycin treatment was observed to shut down LINE-1 gene expression activated by RASER-VP64 and mCh-dCas9, while no significant change was noted for the control group coexpressing LaM8-VP64 and mCh-dCas9 (Fig. 4d).

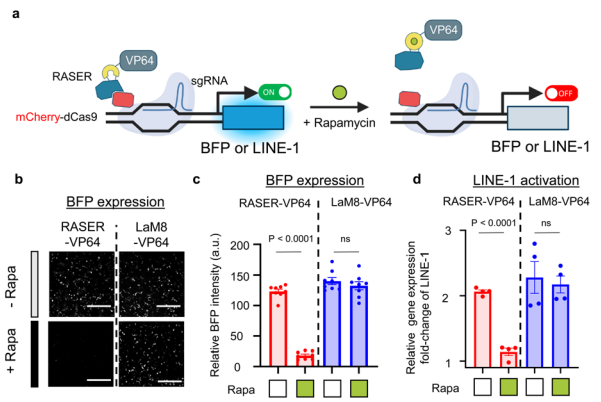

Fig. 4 RASER applied to achieve rapamycin-induced shutdown of customized gene expression. Data are presented as mean ± sem. (a) Cartoon illustrating the design of a rapamycin-switchable split CRISPRa system made of mCherry-dCas9 and RASER-VP64. In the absence of rapamycin, RASER-VP64 interacts with mCh-dCas9 to induce gene expression. Upon rapamycin treatment, RASER-VP64 dissociates from mCh-dCas9 to terminate transcriptional activation. BFP is used as a reporter for dCas9-VP64-mediated transcriptional regulation. (b) Confocal images showing BFP expression in HeLa cells transfected with the rapamycin-activatable CRISPRa system (RASER-VP64 + mCh-dCas9) or the positive control vectors (LaM8-VP64 + mCh-dCas9) before and after overnight rapamycin treatment. Scale bar, 500 μm. (c) Quantification of BFP signals before and after rapamycin treatment (as shown in panel b). $n = 8$ fields of view from three independent assays. (d) Bar graph showing the relative human LINE-1 expression in HEK293T cells, measured by real-time RT-PCR, for cells coexpressing the indicated constructs with specific guide RNAs, compared to the control group with non-targeting guide RNAs. ns, not statistically significant.

Taken together, this rapamycin-triggered dissociation system provides a complementary platform that extends the functional scope of FRB-FKBP-based systems for precise CRISPR regulation in biological applications.

Conclusions

In this study, we leveraged genetically encoded nanobodies that allosterically respond to caffeine (Caffebodies) and rapamycin (Rapabodies) to develop CHASER and RASER, thereby adding new functional capabilities to two popular CIP systems. While the relatively low heterodimerization efficiency of COSMO restricts its use in many biomedical contexts, CHASER provides an alternative with markedly improved performance, as exemplified by CHASER-TrkA, which enabled robust caffeine-induced RTK activation. Our previous work with biCOSMO-L demonstrated that caffeine-induced intramolecular interactions effectively prevent competing intermolecular interactions,[12] thereby explaining CHASER's high heterodimerization efficiency. Although CHASER exhibits slower dissociation kinetics compared to COSMO, this can be advantageous for applications requiring sustained activation, such as prolonged signalling or long-term effector recruitment, where more persistent binding is a strength rather than a limitation.[45] On the other hand, the rapamycin-induced FRB-FKBP system suffers from poor reversibility, making it equally important and complementary to develop a rapamycin-triggered dissociation system. This need is fulfilled by RASER, whose utility was further validated in rapamycin-inducible control of a CRISPRa system.

In conclusion, CHASER and RASER represent a rational strategy to expand the CIP toolbox by reprogramming existing modules through re-engineering of nanobodies, thereby filling critical gaps in current biological and therapeutic applications of these chemogenetic tools. This simple and modular engineering approach circumvents the need to design entirely new CIP chemistries from scratch, which is often costly and time-consuming.

Author contributions

Y. Z., L. H. and T. W. conceived the ideas and directed the work. T. W. and YZ designed the study. T. W., T. N., P. X. C., T.-H.L., M. C. and L. H. performed the experiments. T. W., L. H. and Y. Z. analysed the results. Y. Z., T. N., L. H. and T. W. wrote the manuscript. All the authors contributed to the discussion and editing of the manuscript.

Conflicts of interest

The United States Patent and Trademark Office has granted the design and biomedical application aspect(s) of switchable nanobodies (US12,152,066).

Data availability

The data supporting this article have been included as part of the supplementary information (SI). Supplementary information: supplementary methods and Fig. S1–S6. See DOI: **https://doi.org/10.1039/d5sc05703e**.

Acknowledgements

This work was supported by the National Institutes of Health (R01GM144986 and R21AI174606 to Y. Z.), the Center Prevention and Research Institute of Texas (RP250468 to Y. Z.), the Welch Foundation (BE-1913-20220331 to Y. Z.) and the Leukaemia & Lymphoma Society (to Y. Z.).

Notes and references

1 B. Z. Stanton, E. J. Chory and G. R. Crabtree, Chemically induced proximity in biology and medicine, *Science*, 2018, 359.
2 S. Shui, S. Buckley, L. Scheller and B. E. Correia, Rational design of small-molecule responsive protein switches, *Protein Sci.*, 2023, **32**, e4774.
3 T. Wang, S. Liu, Y. Ke, S. Ali, R. Wang, T. Hong, Z. Liu, G. Ma, T. H. Lan, F. Wang, M. X. Zhu, Y. Huang and Y. Zhou, Repurposing salicylic acid as a versatile inducer of proximity, *Nat. Chem. Biol.*, 2025, **21**, 1444–1456.
4 J. Shen, L. Geng, X. Li, C. Emery, K. Kroning, G. Shingles, K. Lee, M. Heyden, P. Li and W. Wang, A general method for chemogenetic control of peptide function, *Nat. Methods*, 2023, **20**, 112–122.
5 A. Yesbolatova, Y. Saito, N. Kitamoto, H. Makino-Itou, R. Ajima, R. Nakano, H. Nakaoka, K. Fukui, K. Gamo, Y. Tominari, H. Takeuchi, Y. Saga, K. I. Hayashi and M. T. Kanemaki, The auxin-inducible degron 2 technology provides sharp degradation control in yeast, mammalian cells, and mice, *Nat. Commun.*, 2020, **11**, 5701.
6 H. Wang, X. Xu, C. M. Nguyen, Y. Liu, Y. Gao, X. Lin, T. Daley, N. H. Kipniss, M. La Russa and L. S. Qi, CRISPR-Mediated Programmable 3D Genome Positioning and Nuclear Organization, *Cell*, 2018, **175**, 1405–1417.
7 C. Y. Wu, K. T. Roybal, E. M. Puchner, J. Onuffer and W. A. Lim, Remote control of therapeutic T cells through a small molecule-gated chimeric receptor, *Science*, 2015, **350**, aab4077.
8 S. Feng, V. Laketa, F. Stein, A. Rutkowska, A. MacNamara, S. Depner, U. Klingmuller, J. Saez-Rodriguez and C. Schultz, A rapidly reversible chemical dimerizer system to study lipid signaling in living cells, *Angew. Chem., Int. Ed. Engl.*, 2014, **53**, 6720–6723.
9 L. A. Banaszynski, C. W. Liu and T. J. Wandless, Characterization of the FKBP.rapamycin.FRB ternary complex, *J. Am. Chem. Soc.*, 2005, **127**, 4715–4721.
10 V. M. Rivera, T. Clackson, S. Natesan, R. Pollock, J. F. Amara, T. Keenan, S. R. Magari, T. Phillips, N. L. Courage, F. Cerasoli, Jr., D. A. Holt and M. Gilman, A humanized system for pharmacologic control of gene expression, *Nat. Med.*, 1996, **2**, 1028–1032.
11 M. Lee, J. Li, Y. Liang, G. Ma, J. Zhang, L. He, Y. Liu, Q. Li, M. Li, D. Sun, Y. Zhou and Y. Huang, Engineered Split-TET2 Enzyme for Inducible Epigenetic Remodeling, *J. Am. Chem. Soc.*, 2017, **139**, 4659–4662.
12 T. Wang, L. He, J. Jing, T. H. Lan, T. Hong, F. Wang, Y. Huang, G. Ma and Y. Zhou, Caffeine-Operated Synthetic Modules for Chemogenetic Control of Protein Activities by Life Style, *Adv. Sci.*, 2021, **8**, 2002148.
13 O. Dagliyan, D. Shirvanyants, A. V. Karginov, F. Ding, L. Fee, S. N. Chandrasekaran, C. M. Freisinger, G. A. Smolen, A. Huttenlocher, K. M. Hahn and N. V. Dokholyan, Rational design of a ligand-controlled protein conformational switch, *Proc. Natl. Acad. Sci. U. S. A.*, 2013, **110**, 6800–6804.
14 T. H. Lan, N. Ambiel, Y. T. Lee, T. Nonomura, Y. Zhou and J. B. Zuchero, A Chemogenetic Toolkit for Inducible, Cell Type-Specific Actin Disassembly, *Small Methods*, 2025, **9**, e2401522.
15 Y. T. Lee, L. He and Y. Zhou, Expanding the Chemogenetic Toolbox by Circular Permutation, *J. Mol. Biol.*, 2020, **432**, 3127–3136.
16 T. Inoue, W. D. Heo, J. S. Grimley, T. J. Wandless and T. Meyer, An inducible translocation strategy to rapidly activate and inhibit small GTPase signaling pathways, *Nat. Methods*, 2005, **2**, 415–418.
17 R. Pollock, M. Giel, K. Linher and T. Clackson, Regulation of endogenous gene expression with a small-molecule dimerizer, *Nat. Biotechnol.*, 2002, **20**, 729–733.
18 N. Umeda, T. Ueno, C. Pohlmeyer, T. Nagano and T. Inoue, A photocleavable rapamycin conjugate for spatiotemporal control of small GTPase activity, *J. Am. Chem. Soc.*, 2011, **133**, 12–14.
19 J. Shen, G. Zhou and W. Wang, Chemogenetic Tools in Focus: Proximity, Conformation, and Sterics, *Chem. Methods*, 2024, **4**, e202300051.
20 H. Farrants, M. Tarnawski, T. G. Muller, S. Otsuka, J. Hiblot, B. Koch, M. Kueblbeck, H. G. Krausslich, J. Ellenberg and K. Johnsson, Chemogenetic Control of Nanobodies, *Nat. Methods*, 2020, **17**, 279–282.
21 X. Sun, C. Zhou, S. Xia and X. Chen, Small molecule-nanobody conjugate induced proximity controls intracellular processes and modulates endogenous unligandable targets, *Nat. Commun.*, 2023, **14**, 1635.
22 L. He, P. Tan, Y. Huang and Y. Zhou, Design of Smart Antibody Mimetics with Photosensitive Switches, *Adv. Biol. (Weinh)*, 2021, **5**, e2000541.
23 A. A. Gil, C. Carrasco-Lopez, L. Zhu, E. M. Zhao, P. T. Ravindran, M. Z. Wilson, A. G. Goglia, J. L. Avalos and J. E. Toettcher, Optogenetic control of protein binding using light-switchable nanobodies, *Nat. Commun.*, 2020, **11**, 4044.
24 C. Zhou, H. He and X. Chen, Photoactivatable Nanobody Conjugate Dimerizer Temporally Resolves Tiam1-Rac1 Signaling Axis, *Adv. Sci. (Weinh)*, 2024, **11**, e2307549.

25 D. Yu, H. Lee, J. Hong, H. Jung, Y. Jo, B. H. Oh, B. O. Park and W. D. Heo, Optogenetic activation of intracellular antibodies for direct modulation of endogenous proteins, *Nat. Methods*, 2019, **16**, 1095–1100.

26 G. Devereux, S. Cotton, S. Fielding, N. McMeekin, P. J. Barnes, A. Briggs, G. Burns, R. Chaudhuri, H. Chrystyn, L. Davies, A. De Soyza, S. Gompertz, J. Haughney, K. Innes, J. Kaniewska, A. Lee, A. Morice, J. Norrie, A. Sullivan, A. Wilson and D. Price, Effect of Theophylline as Adjunct to Inhaled Corticosteroids on Exacerbations in Patients With COPD: A Randomized Clinical Trial, *JAMA*, 2018, **320**, 1548–1559.

27 T. T. Hansel, R. C. Tennant, A. J. Tan, L. A. Higgins, H. Neighbour, E. M. Erin and P. J. Barnes, Theophylline: mechanism of action and use in asthma and chronic obstructive pulmonary disease, *Drugs Today (Barc)*, 2004, **40**, 55–69.

28 J. S. Khamo, V. V. Krishnamurthy, Q. Chen, J. Diao and K. Zhang, Optogenetic Delineation of Receptor Tyrosine Kinase Subcircuits in PC12 Cell Differentiation, *Cell Chem. Biol.*, 2019, **26**, 400–410.

29 V. V. Krishnamurthy, J. Fu, T. J. Oh, J. Khamo, J. Yang and K. Zhang, A Generalizable Optogenetic Strategy to Regulate Receptor Tyrosine Kinases during Vertebrate Embryonic Development, *J. Mol. Biol.*, 2020, **432**, 3149–3158.

30 M. Ma, P. Bordignon, G. P. Dotto and S. Pelet, Visualizing cellular heterogeneity by quantifying the dynamics of MAPK activity in live mammalian cells with synthetic fluorescent biosensors, *Heliyon*, 2020, **6**, e05574.

31 Z. Cheng, D. Garvin, A. Paguio, P. Stecha, K. Wood and F. Fan, Luciferase Reporter Assay System for Deciphering GPCR Pathways, *Curr Chem Genomics*, 2010, **4**, 84–91.

32 N. T. Nguyen, W. Han, W. M. Cao, Y. Wang, S. Wen, Y. Huang, M. Li, L. Du and Y. Zhou, Store-Operated Calcium Entry Mediated by ORAI and STIM, *Compr. Physiol.*, 2018, **8**, 981–1002.

33 M. Prakriya and R. S. Lewis, Store-Operated Calcium Channels, *Physiol. Rev.*, 2015, **95**, 1383–1436.

34 J. Soboloff, B. S. Rothberg, M. Madesh and D. L. Gill, STIM proteins: dynamic calcium signal transducers, *Nat. Rev. Mol. Cell Biol.*, 2012, **13**, 549–565.

35 Y. Ke, R. Gannaban, J. Liu and Y. Zhou, STIM1 and lipid interactions at ER-PM contact sites, *Am. J. Physiol. Cell Physiol.*, 2025, **328**, C107–C114.

36 Y. Zhou, P. Srinivasan, S. Razavi, S. Seymour, P. Meraner, A. Gudlur, P. B. Stathopulos, M. Ikura, A. Rao and P. G. Hogan, Initial activation of STIM1, the regulator of store-operated calcium entry, *Nat. Struct. Mol. Biol.*, 2013, **20**, 973–981.

37 G. Ma, L. He, S. Liu, J. Xie, Z. Huang, J. Jing, Y. T. Lee, R. Wang, H. Luo, W. Han, Y. Huang and Y. Zhou, Optogenetic engineering to probe the molecular choreography of STIM1-mediated cell signaling, *Nat. Commun.*, 2020, **11**, 1039.

38 J. Abramson, J. Adler, J. Dunger, R. Evans, T. Green, A. Pritzel, O. Ronneberger, L. Willmore, A. J. Ballard, J. Bambrick, S. W. Bodenstein, D. A. Evans, C. C. Hung, M. O'Neill, D. Reiman, K. Tunyasuvunakool, Z. Wu, A. Zemgulyte, E. Arvaniti, C. Beattie, O. Bertolli, A. Bridgland, A. Cherepanov, M. Congreve, A. I. Cowen-Rivers, A. Cowie, M. Figurnov, F. B. Fuchs, H. Gladman, R. Jain, Y. A. Khan, C. M. R. Low, K. Perlin, A. Potapenko, P. Savy, S. Singh, A. Stecula, A. Thillaisundaram, C. Tong, S. Yakneen, E. D. Zhong, M. Zielinski, A. Zidek, V. Bapst, P. Kohli, M. Jaderberg, D. Hassabis and J. M. Jumper, Accurate structure prediction of biomolecular interactions with AlphaFold 3, *Nature*, 2024, **630**, 493–500.

39 M. L. Maeder, S. J. Linder, V. M. Cascio, Y. Fu, Q. H. Ho and J. K. Joung, CRISPR RNA-guided activation of endogenous human genes, *Nat. Methods*, 2013, **10**, 977–979.

40 N. Khajanchi and K. Saha, Controlling CRISPR with small molecule regulation for somatic cell genome editing, *Mol. Ther.*, 2022, **30**, 17–31.

41 B. Zetsche, S. E. Volz and F. Zhang, A split-Cas9 architecture for inducible genome editing and transcription modulation, *Nat. Biotechnol.*, 2015, **33**, 139–142.

42 M. S. Robinson, D. A. Sahlender and S. D. Foster, Rapid inactivation of proteins by rapamycin-induced rerouting to mitochondria, *Dev. Cell*, 2010, **18**, 324–331.

43 C. R. Beck, P. Collier, C. Macfarlane, M. Malig, J. M. Kidd, E. E. Eichler, R. M. Badge and J. V. Moran, LINE-1 retrotransposition activity in human genomes, *Cell*, 2010, **141**, 1159–1170.

44 T. Honda, Y. Nishikawa, K. Nishimura, D. Teng, K. Takemoto and K. Ueda, Effects of activation of the LINE-1 antisense promoter on the growth of cultured cells, *Sci. Rep.*, 2020, **10**, 22136.

45 Y. C. Lin, Y. Nihongaki, T. Y. Liu, S. Razavi, M. Sato and T. Inoue, Rapidly reversible manipulation of molecular activity with dual chemical dimerizers, *Angew. Chem., Int. Ed. Engl.*, 2013, **52**, 6450–6454.